Contract No:

This document was prepared in conjunction with work accomplished under Contract No. 89303321CEM000080 with the U.S. Department of Energy (DOE) Office of Environmental Management (EM).

Disclaimer:

A U.S. DEPARTMENT OF ENERGY NATIONAL LAB • SAVANNAH RIVER SITE • AIKEN, SC • USA

Dissolution Flowsheet for Skull Oxide Generated during U-Mo Alloy Casting for High Performance Research Reactor Fuel

W. E. Daniel

T. S. Rudisill

J. M. Gogolski

April 2022

SRNL-STI-2022-00149, Revision 0

DISCLAIMER

Printed in the United States of America

Prepared for
U.S. Department of Energy

SRNL-STI-2022-00149
Revision 0

Keywords: *Dissolution, U-Mo Skull Oxide, High Performance Research Reactor Fuel*

Retention: *Permanent*

Dissolution Flowsheet for Skull Oxide Generated during U-Mo Alloy Casting for High Performance Research Reactor Fuel

W. E. Daniel
T. S. Rudisill
J. M. Gogolski

April 2022

Savannah River National Laboratory is operated by Battelle Savannah River Alliance for the U.S. Department of Energy under Contract No. 89303321CEM000080.

REVIEWS AND APPROVALS

AUTHORS:

_____
W. E. Daniel, Separation and Actinide Science Date

_____
T. S. Rudisill, Separation and Actinide Science Date

_____
J. M. Gogolski, Separation and Actinide Science Date

TECHNICAL REVIEW:

_____
C. A. Nash, Separation Sciences and Engineering, Reviewed per E7 2.60 Date

APPROVAL:

_____
J. M. Duffey, Manager Date
Separation and Actinide Science

_____
A. P. Fellinger, Crosscutting Pillar Program Manager, Actinide and Separations Science Date

PREFACE OR ACKNOWLEDGEMENTS

The authors would like to acknowledge the support of the SRNL Glass Shop for not only constructing but helping to improve the design of glassware used in the dissolution experiments for the U-10Mo scrap recovery flowsheet development. The Glass Shop was able to modify equipment designs and refabricate needed glassware within a matter of days which allowed the project to proceed on schedule.

EXECUTIVE SUMMARY

The Savannah River National Laboratory was requested to develop dissolution flowsheets for high assay low enriched U scrap generated during the fabrication of high performance research reactor fuel. The scrap streams include U-10Mo and U-10Mo-Zr foils, rejected Al-clad fuel plates, and skull oxide from casting molds. Flowsheets for the dissolution of the U-10Mo-Zr foils and Al-clad U-10Mo-Zr mini-plates received from BWX Technologies, Inc were developed and demonstrated in the first phase of this project. In the second phase (this work), the skull oxide from a U-10Mo casting mold was obtained from the Y-12 National Security Complex (Y-12) and small-scale experiments were performed to demonstrate dissolution flowsheets.

The skull oxide from the Y-12 casting operation was dissolved using the optimized conditions demonstrated for the dissolution of the U-10Mo-Zr foil and Al-clad U-10Mo-Zr mini-plates targeting final U concentrations of both 20 and 50 g/L. The flowsheet recommendations were based on the use of sufficient 4 M HNO_3 at the boiling point to achieve a final acid concentration greater than approximately 3.5 M when targeting either U concentration. For dissolutions targeting 50 g/L U, 0.5 M Fe should be added to the solution to prevent the precipitation of uranyl molybdate. Following dissolution, the undissolved solids (UDS) must be filtered to remove the insoluble graphite from the casting mold. The UDS require rinsing with fresh dissolving solution to prevent the loss of U from the interstitial liquid.

Material balance and recovery efficiency data from the experiments confirm that the U in the skull oxide was soluble in the HNO_3 solutions used to perform the dissolutions. The UDS remaining from experiments targeting 20 and 50 g/L U were 4-7% of the mass of the source material which was approximately equal to the amount of graphite in the skull oxide (5.1 wt %) based on an analysis provided by Y-12. Uranium material balance closures were nominally 100% and the amount of U remaining in the UDS was less than approximately 0.5% and was less than 0.1% for the experiment targeting a final U concentration of 50 g/L. The UDS following dissolution of the skull oxide can be discarded as a low level waste without any significant loss of U.

The offgas generation and composition from the skull oxide dissolutions were measured by Raman spectroscopy. There was no detectable H_2 in the offgas stream from the casting skull dissolutions which is consistent with the dissolution of U oxides. The offgas consisted of 100% NO with an approximate peak generation rate of 0.3 cm^3/min (0 °C, 1 atm) per gram of skull oxide. It took about 19 minutes to dissolve each gram of skull oxide for the dissolution targeting 20 g/L U and about 10 minutes to dissolve each gram of skull oxide targeting 50 g/L U based on the NO generation. The presence of the Fe in the solution likely increased the dissolution rate for the experiment targeting 50 g/L U.

TABLE OF CONTENTS

LIST OF TABLES

LIST OF FIGURES

LIST OF ABBREVIATIONS

ANL	Argonne National Laboratory
ATR	Advanced Test Reactor
BWXT	BWX Technologies, Inc.
HEU	highly enriched U
HFIR	High Flux Isotope Reactor
HIP	hot isostatic pressing
ICPES	inductively-coupled plasma emission spectrometry
ICPMS	inductively-coupled plasma mass spectrometry
LECO	Laboratory Equipment Corporation
LEU	low enriched U
M^3	Material Management and Minimization
MIT	Massachusetts Institute of Technology
MURR	University of Missouri Research Reactor
NBSR	National Bureau of Standards Reactor
NNSA	National Nuclear Security Administration
SRNL	Savannah River National Laboratory
SRS	Savannah River Site
UDS	undissolved solids
USHPRR	United States High Performance Research Reactor
XRD	X-ray diffraction
Y-12	Y-12 National Security Complex

1.0 Introduction

1.1 Background

The National Nuclear Security Administration (NNSA) Office of Material Management and Minimization (M^3) United States High Performance Research Reactor (USHPRR) project is developing a low enriched U-10Mo fuel to replace the highly enriched U (HEU) fuels currently being used in the U.S. high performance reactors. The USHPRR's include the Massachusetts Institute of Technology (MIT) Reactor, University of Missouri Research Reactor (MURR), National Bureau of Standards Reactor (NBSR) at the National Institute of Standards and Technology, Advanced Test Reactor (ATR) at the Idaho National Laboratory, and High Flux Isotope Reactor (HFIR) at Oak Ridge National Laboratory. The proposed baseline fuel has an Al cladding like the present generation of fuel; however, the fuel fissionable component consists of a low enriched U-10Mo monolithic alloy with a thin layer of Zr between the fuel core and the cladding. The USHPRR Project team is working with the national laboratory complex to develop and qualify the low enriched U (LEU) fuel to facilitate the research reactor conversions starting with the Nuclear Regulatory Commission licensed HPRR's, (i.e., MIT, MURR and NBSR reactors).[1]

The U-10Mo fuel design is based on a monolithic U-10Mo alloy, sealed in Al cladding (alloy Al-6061), with a diffusion/bonding Zr interlayer. A schematic of a foil-type element under consideration is shown in Figure 1-1. The new LEU fuel design has a much higher U density than in the conventional HEU dispersion fuel designs, which is required to convert the USHPRR's to LEU fuels.[1]

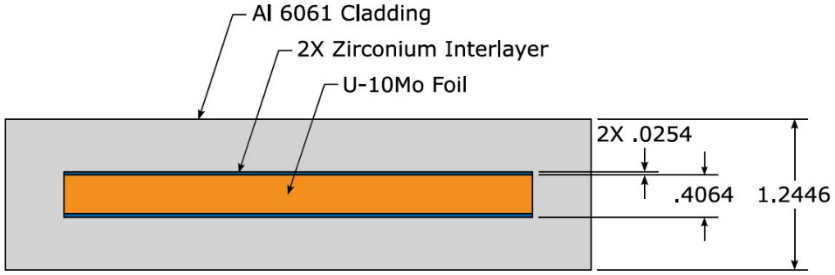

Figure 1-1. Schematic Diagram of a Typical U-10Mo Fuel Plate (not to scale-units in millimeters)

The casting operations used to produce the U-10Mo alloy and the fuel fabrication processes result in the generation of scrap streams containing LEU which must be recovered. Figure 1-2 provides a list of the scrap streams generated in both casting and fuel fabrication and their disposition paths. The scrap streams are defined in Table 1-1.[1] The aqueous recovery processes proposed by Dunn et al. for the U-Mo scrap streams are based on the dissolution of the materials using HNO_3-based flowsheets. The Al cladding on plates that do not meet specification after the hot isostatic pressing (HIP) operation may be initially removed using a caustic solution (e.g., NaOH). Other materials such as fluoride or Fe(III) may be added to the dissolving solution to increase the solubility of other components of the fuel (e.g., Zr and Mo).[1]

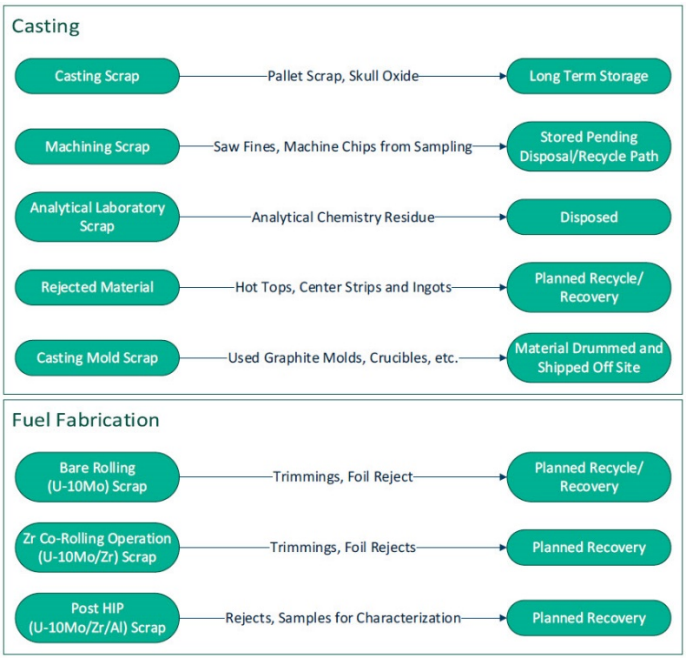

Figure 1-2. Scrap Streams from USHPRR Fuel Fabrication and Planned Disposition

Table 1-1. Definition of Scrap Streams

Scrap Stream	Definition
Analytical Chemistry Residue	Liquid residues remaining after the analytical chemistry analyses are completed
Rejected Center Strip	Strip of material between the two ingots that is drilled to supply material for chemical analysis
Crucible	Graphite vessel in which the materials are melted for casting
Trimmings	Portion of co-rolled plates that are removed due to imperfections
Reject Foils	Foils that do not meet specification and cannot be accepted with a non-conformance report
Hot Tops	Top portion of the casted plate that is removed after casting
Ingots	Portion of the casted plate that is removed for further processing (rolling, etc.)
Machine Chips from Sampling	Machining fines remaining after samples of the center strip are removed with a drill for chemical analysis
Pallet Scrap	Material that leaks out or spills out of mold during a pour (which is heavily oxidized and carbon-contaminated with non-U elements)
Graphite Molds	Graphite material such as mold housing, plates, etc. used in the casting process
Rejects (Post HIP)	Plates that do not meet specification after the HIP operation (Zr coated foils encased in Al)
Characterization Samples	Portions of center strip that are removed with a drill for analytical chemistry
Saw Fines	Material that remains after the sawing/machining operations
Skull	Material that remains in the crucible after the molten material is poured into the mold housing
Trimming	Pieces of foils that are removed after bare rolling or co-rolling

1.2 Dissolution of U-10Mo Alloys

Dissolution flowsheets have been demonstrated for both U-Mo reactor fuels and the scrap generated from the fabrication of fuel from U-Mo alloys. Stepinski et al. summarized previous work used to develop dissolution flowsheets for irradiated U-Mo fuels as part of the NNSA's Fuel Fabrication Capability Project in 2008.[2] The document provides a comprehensive review of U-Mo dissolution technology up to this date. Stepinski et al. and Jerden et al. used this information as the basis for flowsheet recommendations for the dissolution of U-Mo scrap generated during the fabrication of USHPRR fuels.[3,4] Researchers at Argonne National Laboratory (ANL) performed small-scale dissolutions using 0.2 to 1.2 g of U-10Mo, U-8Mo-Zr, and U-10Mo-Zr foils to demonstrate flowsheets for the dissolution of HPRR fuel fabrication scrap.[5-7] The dissolution of off-specification fuel plates was simulated by dissolving small pieces of an Al-6061 alloy prior to the U-Mo-Zr foil. In more recent studies, Daniel et al.[8] demonstrated flowsheets for the dissolution of U-10Mo-Zr foils and Al-clad U-10Mo-Zr mini-plates resulting in both 20 and 50 g/L U solutions. A flowsheet was also demonstrated for the removal of the Al-cladding from the mini-plates using a NaOH solution containing $NaNO_3$ prior to the subsequent dissolution of the U-10Mo-Zr foil.

The most important consideration in designing a U-Mo dissolution process is the limited solubility of Mo in $UO_2(NO_3)_2$ solutions. An extensive study on the solubility of Mo in nitrate-based media in the presence of $Fe(NO_3)_3$ and other metal salts was performed by Faugeras.[9] The solubility of Mo as a function of the U and HNO_3 concentrations is shown in Figure 1-3.

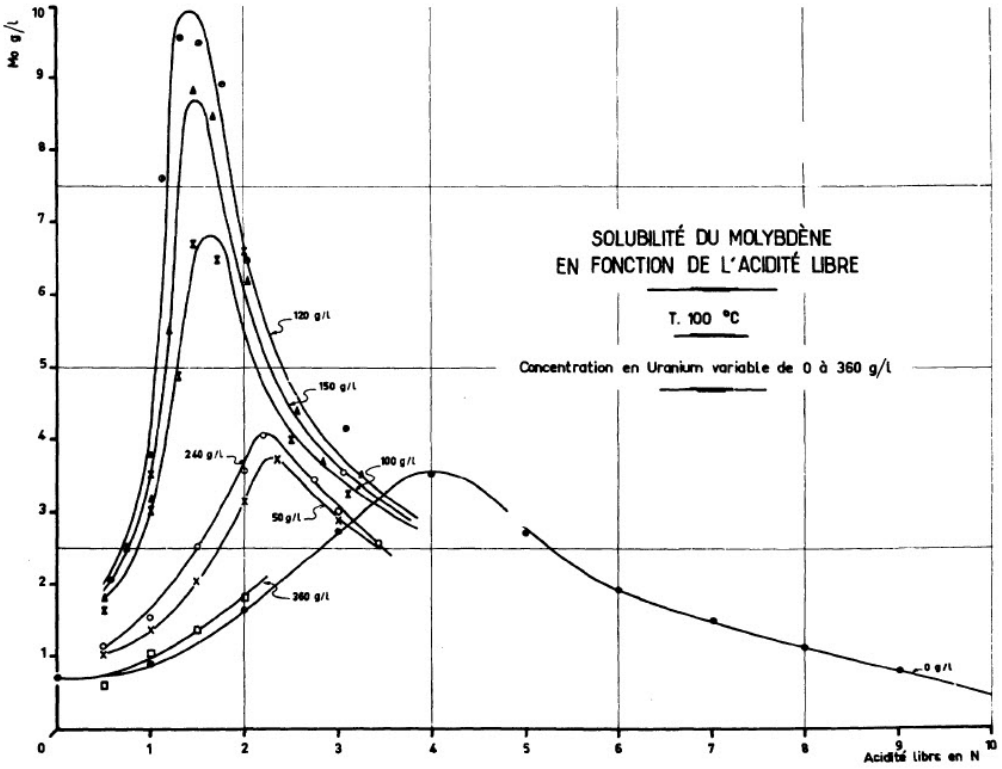

Figure 1-3. Solubility of Mo in HNO_3 Solutions Containing U

Faugeras et al. also completed extensive studies on the solubility of Mo in $UO_2(NO_3)_2$ – HNO_3 solutions in the presence of 0.25-1.5 M $Fe(NO_3)_3$. Data from this study for solutions containing 0.5 M $Fe(NO_3)_3$ are plotted in Figure 1-4.[9] The increased solubility of Mo can be attributed to the formation of a negatively charged Fe–Mo complex which prevents precipitation of uranyl molybdate.[10] Based on the increased solubility of Mo in HNO_3 solutions containing U and Fe, one strategy for dissolving U-10Mo scrap to

higher terminal U concentrations and lower terminal HNO_3 concentrations is the addition of $Fe(NO_3)_3$ to the dissolving solution. However, this dissolution strategy must be balanced against increasing nuclear safety concerns with increasing ^{235}U concentrations and the generation of more waste from the addition of Fe(III). The Mo solubility data from Faugeras et al.[9] for 0 and 0.5 M Fe for various U concentrations at 100 °C was combined in Figure 1-5 to show how the HNO_3 and Fe(III) concentrations impact Mo solubility.

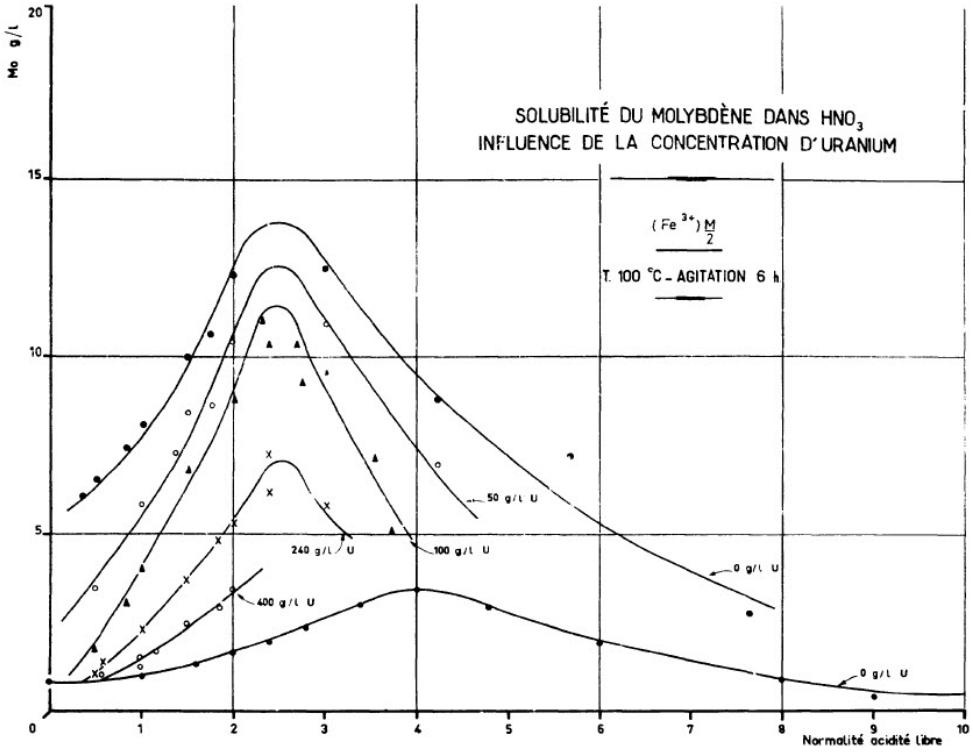

Figure 1-4. Solubility of Mo in HNO_3 Solutions Containing U and 0.5 M $Fe(NO_3)_3$

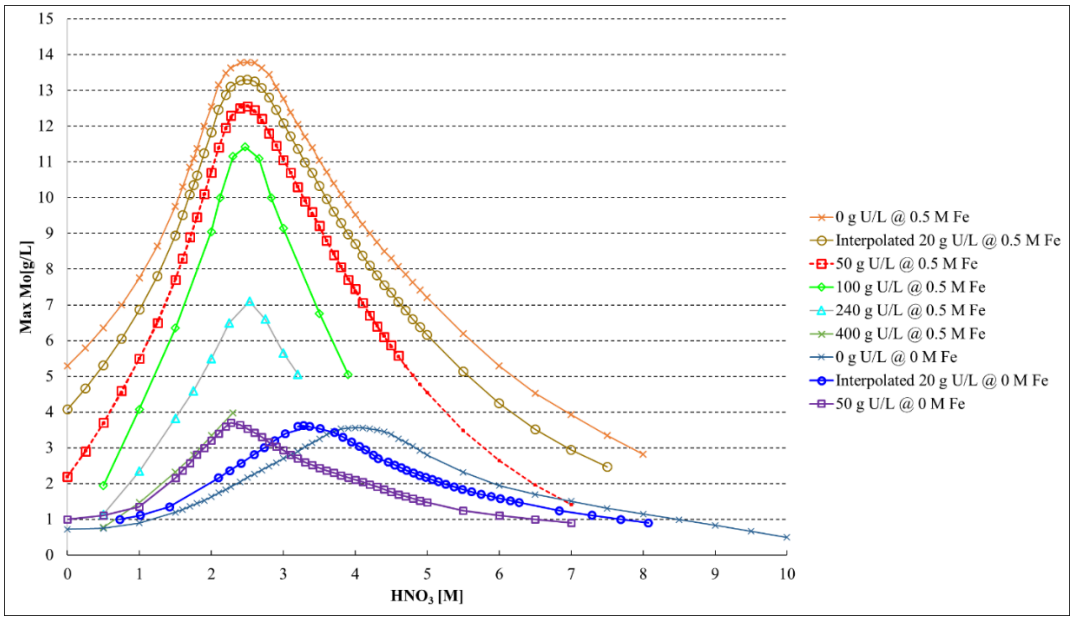

Figure 1-5. Solubility of Mo in HNO_3 Solutions Containing U and 0 and 0.5 M $Fe(NO_3)_3$

The presence of other nitrate salts such as $Al(NO_3)_3$ also has a significant effect on the solubility of Mo in HNO_3 solutions. Figure 1-6 shows data measured by Faugeras et al. for Mo solubility in 1 M HNO_3 as a function of the total nitrate concentration.[9] Separate curves for $Fe(NO_3)_3$, $UO_2(NO_3)_2$, and $Al(NO_3)_3$ are provided. The scrap streams generated in both U-10Mo casting and fuel fabrication upon dissolution may contain other metal nitrate salts (e.g., Al, Zr, Fe, and others) besides U which must be addressed during development of the dissolution flowsheets.

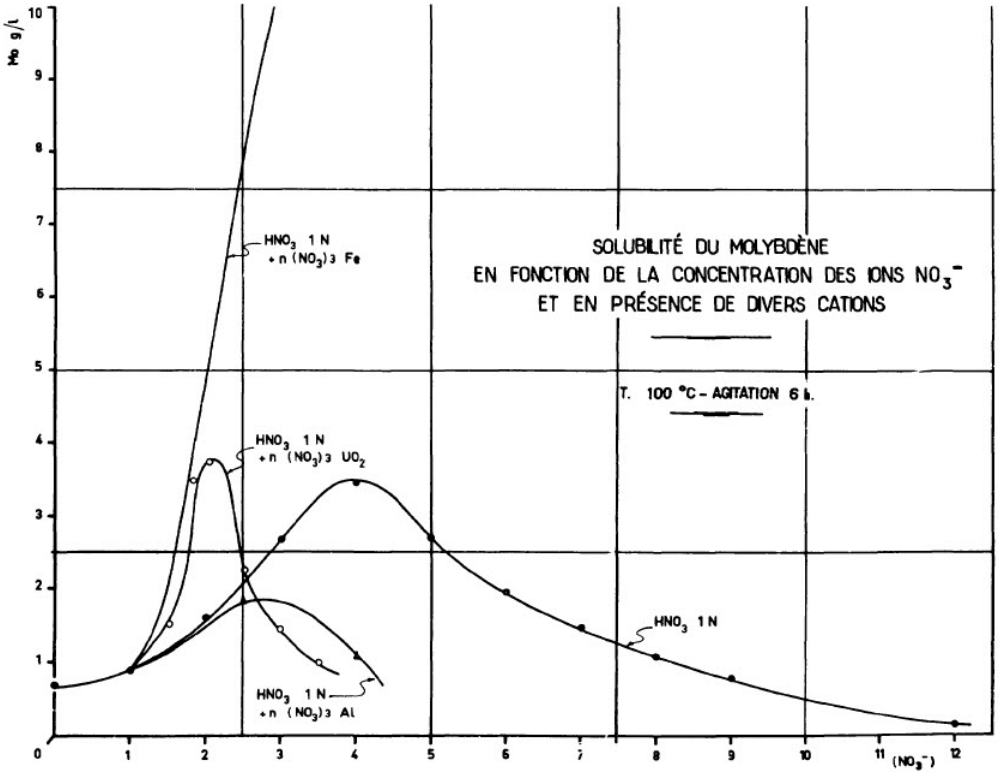

Figure 1-6. Solubility of Mo in 1 M HNO_3 Containing Other Metal Nitrates

1.3 Objectives

The Savannah River National Laboratory (SRNL) was requested to develop dissolution flowsheets for casting and fuel fabrication scraps representative of streams shown in Figure 1-2 which will be processed for U recovery.[11,12] The casting scrap includes the U-10Mo skull oxide from alloy preparation. Skull oxide material generated during a U-10Mo casting was shipped from the Y-12 National Security Complex (Y-12) to SRNL for use in dissolution tests. Fuel fabrication scraps including U-10Mo-Zr foil and Al-clad U-10Mo-Zr mini-plates were obtained from BWX Technologies, Inc. and were previously used for dissolution flowsheet development.[8] The skull oxide material was used in a series of experiments to demonstrate flowsheets which can be used to safely and efficiently dissolve the oxide material for subsequent U recovery. The dissolution processes were designed to accommodate downstream processing without significant solution adjustments to the extent possible. Following dissolution, the U will be purified and recovered as a $UO_2(NO_3)_2$ solution using a modified PUREX process.

2.0 Experimental Procedure

2.1 U-10Mo Casting Skull

The skull oxide from a U-10Mo casting was received from Y-12 to develop and demonstrate optimized dissolution flowsheets. The flowsheets were designed to prevent the generation of solids during dissolution and to keep the solution stable from precipitation once the dissolution of the oxide material was complete. A photograph of the U-Mo oxide casting skull received from Y-12 is shown in Figure 2-1.

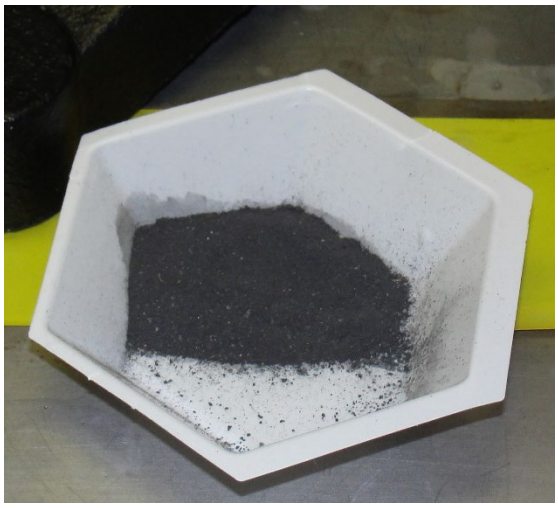

Figure 2-1. Casting Skull from U-10Mo Alloy Production at Y-12

After the skull oxide was received at SRNL, Y-12 provided characterization data from samples removed from the bulk material prior to the shipment. Elemental data were provided from both inductively-coupled plasma emission and mass spectroscopy (ICPES and ICPMS) analyses. The presence of carbon in the oxide material was also established using a LECO carbon analyzer. The concentrations measured by Y-12, the elemental composition, and the estimated composition of the material on an oxide basis are provided in Table 2-1. The presence of C and Er_2O_3 are attributed to the graphite mold used for the U-10Mo casting. An Er_2O_3 coating is applied to the graphite mold as a release agent for the U-10Mo ingot prior to casting. When the skull oxide is scraped from the casting mold, the oxide material is contaminated with both graphite (i.e., C) and Er_2O_3.

Table 2-1. Composition of Skull Oxide Based on Y-12 Analyses

Element	Concentration	Composition(1)	Oxide	Composition
---	(µg/g)	(wt %)	---	(wt %)
C	52200	5.97	C	5.11
Er	200000	22.89	Er_2O_3	22.39
Mo	22750	2.60	MoO_3	3.34
Sn	60	0.02	SnO_2	0.01
U	598667	68.52	U_3O_8	69.15

(1) Oxide-free basis

2.2 Skull Oxide Dissolution

The objective for the flowsheets demonstrated for the skull oxide material was to use the same conditions as demonstrated for the dissolution of the U-10Mo-Zr foil and Al-clad U-10Mo-Zr mini-plates.[8] The flowsheet recommendations for the dissolution of the foil and mini-plates were to use a sufficient volume of 4 M HNO_3 at the boiling point of the solution to achieve a final acid concentration greater than

approximately 3.5 M when targeting either 20 or 50 g/L U. For dissolutions targeting 50 g/L U, 0.5 M Fe (as $Fe(NO_3)_3$) should be added to the solution to prevent the precipitation of uranyl molybdate. However, since the skull oxide material contained graphite which would be mostly insoluble in the HNO_3 solution, there was concern that all of the U could not be leached from the undissolved solids (UDS). To address this concern, an initial scoping experiment (Exp. 181) was performed targeting a terminal U concentration of 20 g/L in 300 mL of solution to evaluate the amount of U which leached from the UDS or if the skull oxide required pretreatment (e.g., calcination to remove graphite) prior to the dissolution process. Following the initial dissolution, two additional experiments (Exp. 183 and 184) were performed targeting final U concentrations of 20 and 50 g/L. The offgases generated during these dissolutions were also characterized by Raman spectroscopy to measure the hydrogen generation rates. The conditions used during each dissolution experiment are summarized in Table 2-2.

Table 2-2. Summary of Conditions Used for Skull Oxide Dissolution Experiments

Exp. No.	U Target	Object (Evaluate)	Initial HNO_3	$Fe(NO_3)_3$	Acid Volume	Oxide Dissolved
---	(g/L)	---	(M)	(M)	(mL)	(g)
181	20	U-Mo oxide solubility and UDS	4.00	0	300	10.0036
183	20	U-Mo oxide solubility and offgas generation	4.00	0	150	5.0058
184	50	U-Mo oxide solubility and offgas generation	4.50	0.5	150	12.8148

The initial concentration of HNO_3 required to dissolve the skull oxide can be estimated using the dissolution stoichiometry shown in Table 2-3 for the major metal components of the material. For the scoping experiment, an estimated 0.11 mole of HNO_3 is required to dissolve the oxides based on the mass given in Table 2-2 and the composition provided in Table 2-1. If a final concentration of 3.5 M is targeted, an estimated 1.16 moles of HNO_3 are required. Since the exact dissolution stoichiometry may vary from the idealized equations provided in Table 2-3 and other reactions (e.g., digestion of graphite and dissolution of minor metal components) may consume a small amount of HNO_3, an initial solution containing 4 M HNO_3 was used for the dissolution. A similar calculation was performed to determine the HNO_3 concentration used for the dissolution of the skull oxide targeting a final U concentration of 50 g/L.

Table 2-3. Dissolution Stoichiometry to Estimate Final HNO_3 Concentration

Dissolution Stoichiometry	Mole HNO_3/Mole Oxide
$U_3O_8 + 8HNO_3 \rightarrow 3UO_2(NO_3)_2 + 2NO_2 + 4H_2O$	8
$Er_2O_3 + 6HNO_3 \rightarrow 2Er(NO_3)_3 + 3H_2O$	6
$MoO_3 + HNO_3\ 3H_2O \rightarrow MoO_2(OH)(H_2O)NO_3$[13]	1

In the experiments performed with offgas characterization (Exp. 183 and 184), the dissolutions were completed using a smaller dissolving vessel (compared to Exp. 181) to reduce the vapor head space. Low offgas generation rates were expected during the dissolution of the skull oxide and a reduced vapor space would improve the ability to measure the offgas components. The smaller vessel limited the solution volume to 150 mL. Therefore, for a target 20 g/L U solution (Exp. 183), 5.0 g of the U-Mo oxide material was targeted in 150 mL of 4 M HNO_3 to maintain the final HNO_3 concentration above 3.5 M. For a target 50 g/L U solution (Exp. 184), 150 mL of 4.5 M HNO_3 containing 0.5 M Fe were used. A higher HNO_3 concentration was required due to the increase in the U concentration (50 g/L versus 20 g/L) and 0.5 M Fe was added to prevent the unwanted precipitation of uranyl molybdate.

2.3 Dissolving System

Small-scale dissolution experiments were performed using laboratory-scale glassware similar to the equipment shown in Figure 2-2. The dissolving vessel was fabricated from a modified 300-mL round-bottom flask (Figure 2-3) with penetrations for a condenser, reagent addition, thermocouple, and gas purge. The bottom of the flask was flattened slightly to facilitate heating and agitation using a hot plate/stirrer with a magnetic stir bar. The solution temperature was controlled using an external thermocouple monitored by the hot plate.

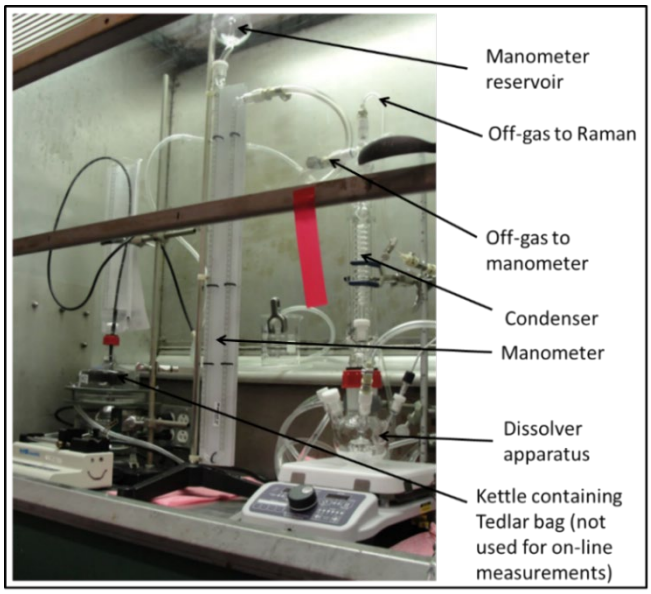

Figure 2-2. Dissolver Setup with Online Raman Offgas Analysis

Figure 2-3. Dissolver Apparatus for Casting Skull Dissolution

Offgas exiting the dissolving vessel was analyzed by Raman spectroscopy using a probe inserted into a flow cell just after the condenser. Chilled water (at 3-4 ˚C) was circulated through the condenser during the dissolution to remove water vapor and other condensable gases from the offgas stream. Condensable water must not enter the Raman cell to avoid interference with the concentration measurements. The offgas leaving the condenser passed through the cell containing the Raman probe and terminated in a bubbler (beaker containing 700 mL or 3.5 in. of deionized water). The Raman spectrometer was used to measure non-condensable gases such as H_2, N_2, O_2, CO_2 NO, N_2O, and NO_2 in real time during an experiment. A known flowrate of CO_2 was added to the dissolving vessel during a dissolution to determine the offgas generation rate using the measured concentration of CO_2 in the offgas stream. A manometer, also connected to the offgas flow cell, was used as a pressure relief device and provided a measure of the system pressure. The bubbler prevented air in-leakage from the vent side of the system.

2.3.1 Raman Spectrometer

The Raman spectrometer is a GasRaman NOCH-1 spectrograph with a 532 nm DPSS laser, a high Rayleigh rejection fiber optic probe, and a high-resolution spectrometer achieving up to ~8 cm^{-1} average optical resolution with spectral coverage from ~250 to 4,200 cm^{-1}. The Raman non-intrusively analyzes the offgas from a dissolution experiment through a quartz window using the excitation of a laser passing through a fixed portion of the offgas stream. The Raman scattering technique identifies and measures the concentration of gases in the offgas stream. The Raman spectrometer was also calibrated using the standard gases shown in Table 2-4. The Raman spectrometer measures the concentrations of the offgas species approximately every 12-13 seconds. Since the Raman spectrometer directly measures the concentrations in the offgas stream, there is no time lag between the measurement and the offgas concentration reading as compared to removing a sample from the offgas stream for analysis by mass spectrometry or gas chromatography. The Raman spectrometer was controlled by and data was logged using a computer running EZRamanReader v8.3.9 software and an Excel spreadsheet.

To calculate offgas generation rates in experiments in which the Raman spectrometer was used to characterize the offgas, a CO_2 tracer gas was metered into the system through a flow controller at a set rate (nominally 7 cm^3/min @ 0 °C, 1 atm). The CO_2 tracer gas had a purity ≥ 99.99% CO_2. Carbon dioxide was chosen as the tracer gas instead of N_2 since it was not expected that the graphite would oxidize to form CO or CO_2.[14] The total offgas rate was then calculated by dividing the set input rate by the measured CO_2 concentration in the offgas.

Table 2-4. Calibration Gases for Raman Analyzers

Supplier	Gas	Ar	N_2	N_2O	NO_2	NO	O_2	H_2
		(vol %)	(vol %)	(vol %)	(vol %)	(vol %)	(vol %)	(vol %)
Air Liquide	20% N_2O-80% Ar	80.00	—	20.00	—	—	—	—
Liquid Technology	5% NO_2-20% O_2-75% Ar	74.89	—	—	4.98	—	20.13	—
Air Liquide	20% NO-80% Ar	80.00	—	—	—	20.00	—	—
Air Liquide	5% N_2-10% H_2-85% Ar	85.00	5.00	—	—	—	—	10.00
SRNL	Ar	≥ 99.995	—	—	—	—	—	—
SRNL	N_2(1)	—	99.9	—	—	—	—	—
SRNL	Air(1)	0.94	78.03	—	—	—	20.99	—

(1) Purity was not measured; the Ar was supplied from SRNL facility gases

2.3.2 Raman Spectrometer Calibration and Sampling Method

The Raman spectrometer was calibrated using the set of calibration gases shown in Table 2-4for the intensities (or quantities) of the calibration gases. The wavelengths for the various calibration gases are

known and remain fixed. Air, 99.9 vol % CO_2, and/or a 2.67 vol % H_2 gas (balance Ar) were analyzed using the Raman spectrometer before and after each experiment. If the calibration checks were off for these gases, the Raman calibration model was then adjusted for those gases after the run to ensure an accurate calibration throughout the dissolution.

The Raman data should sum to 100°vol %. A notable exception is for the 2.67 vol % H_2 gas balanced with 97.33 vol % Ar; Argon is not detectable by the Raman spectrometer. Due to the noise in the Raman signal, raw readings that were less than zero were fixed to zero. In addition, the raw readings were re-baselined to zero by subtracting out average values representing zero. The gas readings for H_2, NO_2, N_2, O_2, N_2O, NO, CO_2, CO, H_2O, and NH_3 are then normalized to 100% except for the 2.67 vol % H_2 gas.

The total offgas flow is calculated from the fixed normalized sum of the CO_2 and CO concentrations divided into the CO_2 tracer flow rate coming into the system. The noise in the concentrations measured by the Raman spectrometer propagates into the total offgas flow rate so moving averages of the total offgas flow rates were performed using equation 1:

$$\text{Offgas flow rate}_{t_i}(\text{cm}^3/\text{min}) = \frac{\sum_{k=t_{i-3}}^{t_{i+3}} \text{Offgas flow rate}_k}{7} \quad (1)$$

where Offgas flow rate = offgas generated by the dissolution in cm^3/min
t_i = time at integer time step i
k= integer time step t_{i-3}, t_{i-2}, t_{i-1}, t_i, t_{i+1}, t_{i+2}, and t_{i+3}

To estimate the variability of the concentrations measured by Raman spectroscopy, the pre-run check values were compared to the standard values for all the experiments. The standard deviations of the measured concentrations with respect to the calibrated concentrations for the data were calculated for each experiment. These standard deviations were then doubled to get an idea of the variability (at an approximate 95% confidence interval) in the Raman spectroscopy concentration measurements. Table 2-5 and Table 2-6 show the standard deviation of the measured concentrations with respect to their calibrated values for the two offgas experiments. For the H_2 gas, the 2σ values or twice the standard deviation is < 0.75 vol %. The 2σ values for CO_2 and N_2 are < 3.0 vol % and the 2σ values for O_2 was < 5.0 vol %.

Table 2-5. Standard Deviation of Raman Concentrations with Respect to Calibrated Values for Exp. 183

Gas	Standard Deviation (σ)	2*Standard Deviation (2σ)
	(vol %)	(vol %)
CO_2	0.57	1.14
N_2	0.75	1.50
O_2	2.46	4.92
H_2	0.30	0.60

Table 2-6. Standard Deviation of Raman Concentrations with Respect to Calibrated Values for Exp. 184

Gas	Standard Deviation (σ)	2*Standard Deviation (2σ)
	(vol %)	(vol %)
CO_2	0.86	1.72
N_2	1.34	2.68
O_2	1.76	3.52
H_2	0.36	0.72

2.4 Quality Assurance

A Functional Classification of Safety Significant was applied to this work based on the Task Technical and Quality Assurance Plan.[12] Analytical measurement systems with a General Service functional classification were used to collect data during the development of flowsheets for the dissolution of the U-10Mo casting skull. Chemical reagents used in experiments and sample preparation were purchased at levels 2 or 3. Standards used for analytical measurements were traceable to NIST or equivalent per manual 1Q, 2-7 section 5.2.3.

To match the requested functional classification, this report received technical review by design verification. Requirements for performing reviews of technical reports and the extent of review are established in manual E7, 2.60. SRNL documents the extent and type of review using the SRNL Technical Report Design Checklist contained in WSRC-IM-2002-00011, Rev. 2.

3.0 Results and Discussion

3.1.1 U-10Mo Casting Skull Dissolution

Since the skull oxide material contained graphite from the Y-12 casting mold which would be mostly insoluble in HNO_3, there was concern that all of the U could not be leached from the UDS. For this reason, an initial scoping experiment (Exp. 181) was performed to evaluate the extent of the U dissolution. In this experiment, 10.0036 g of U-10Mo casting skull was dissolved in 300 mL of 4 M HNO_3 (to keep the final HNO_3 concentration above 3.5 M). These values were expected to give a final solution of 19.5 g/L U in 3.6 M HNO_3. The solution still looked black after 30 minutes of boiling and appeared to have more carbon than expected from the Y-12 characterization (Table 2-1). The solution was cooled and 8.71 g of KF were added to the solution to ensure all the oxides dissolved. The dissolution was resumed by heating the solution back to boiling. After 30 more minutes at boiling the solution appeared to have formed more solids so 22.51 g of $Al(NO)_3 \cdot 9H_2O$ were added to complex the fluoride to prevent the precipitation of U fluorides. The solution was then boiled for an additional hour. After heating was stopped, the solution still appeared black (Figure 3-1). Mixing was stopped to help assess the amount of undissolved material. Most of the solids settled to the bottom of the beaker after about 16 hours. The yellow solution color indicated that a significant amount of the U had dissolved (Figure 3-2).

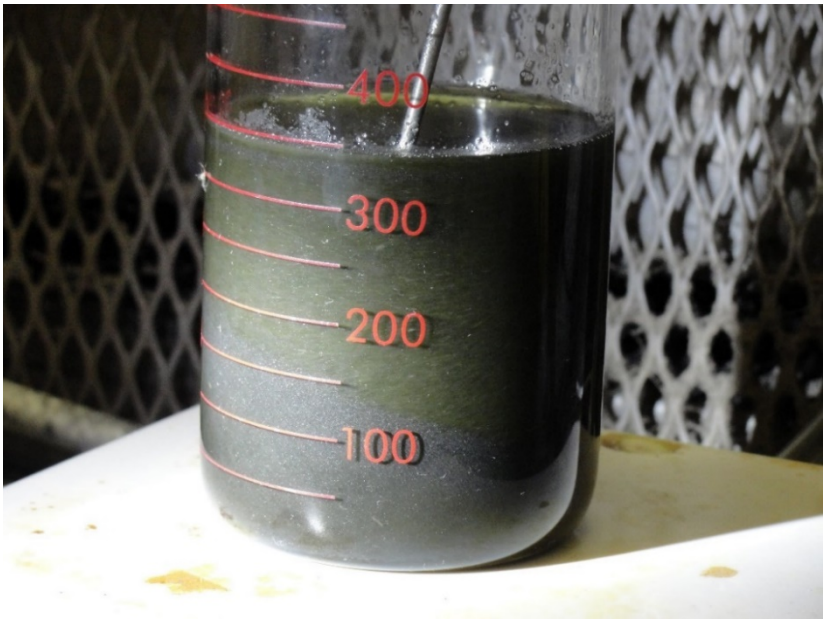

Figure 3-1. Exp. 181 Solution after KF and $Al(NO)_3 \cdot$Addition and Boiling for >1 hour

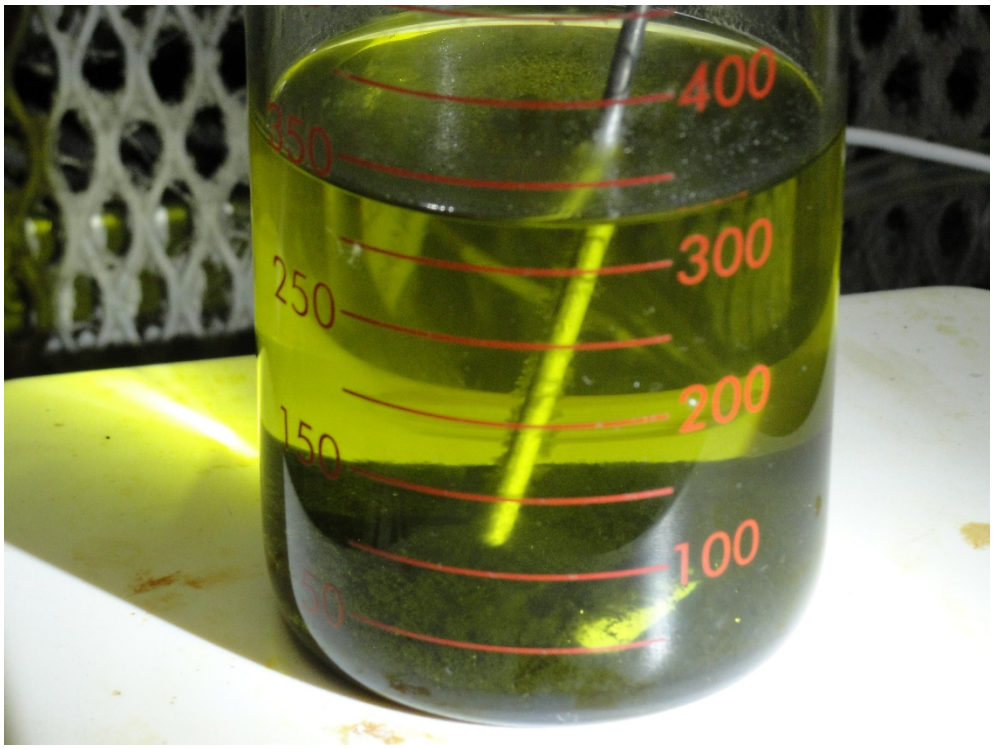

Figure 3-2. Exp. 181 Solution after Sitting for approximately 16 hours

The solution from Exp. 181 was decanted and filtered to remove all of the solids (Figure 3-3). The filtered solids were washed with 4 M HNO_3 to remove residual uranyl nitrate and then analyzed to determine the amount of U dissolved. Due to the addition of KF and $Al(NO_3)_3$ to the dissolving solution, the desired HNO_3 concentration (3.5 M) in the filtrate was reduced to 3.22 M. Additionally, the dendritic precipitant on the thermocouple (Figure 3-2) was analyzed by X-ray diffraction (XRD) and found to be the double salt potassium hexafluorosilicate-potassium nitrate ($K_2SiF_6 \cdot KNO_3$).[15] This compound may be an indication of excess potassium fluoride in solution. The silicon likely originated from hydrofluoric acid attack on the glassware.

Figure 3-3. Exp. 181 Decanted Solution in Filter Cup

Based on the scoping experiment, another dissolution (Exp.183) was performed by dissolving 5.01 g of the U-10Mo casting skull in 150 mL of 4 M HNO_3, targeting a 20 g/L U solution with a final HNO_3 concentration above 3.5 M. In previous work, it was determined that a final HNO_3 concentration between 3.5 and 4.0 M was acceptable in terms of avoiding molybdate precipitates.[8] The final measured free acid for Exp. 183 was 3.6 M which was acceptable. In a third dissolution (Exp. 184), a 50g/L U concentration was targeted by dissolving 12.8 g of skull oxide in 150 mL of 4.5 M HNO_3. A higher initial HNO_3 concentration was required to dissolve to the higher U concentration (50 g/L instead of 20 g/L U). In Exp. 184, 0.5 M Fe(III) (as $Fe(NO_3)_3 \cdot 9H_2O$) was added to the solution to prevent the unwanted precipitation of uranyl molybdate. The final measured free acid concentration for Exp. 184 was 3.6 M HNO_3 which was in the target range. There was UDS associated with each dissolution (as the skull oxide contained approximately 5 wt % graphite), so the solids from all experiments were digested and analyzed. Material balances for each dissolution were performed to evaluate the recovery of U and other elements in the filtrate and UDS streams. The material balances are discussed in the following section.

3.1.2 U-10Mo Casting Skull Material Balances

To close a material balance around each dissolution, the original casting skull from Y-12 was analyzed by the SRNL Analytical Characterization and Sample Management group to confirm the elemental composition of the oxides being dissolved. The casting skull was digested by an alkali-fusion method to solubilize refractory metals and subsequently dissolved in a solution containing HNO_3 and hydrogen peroxide. The solution was analyzed by ICPMS to measure the concentrations of the elements of interest. The elemental concentrations for the skull oxide are shown in Table 3-1 along with the predicted masses of each element dissolved in Exp. 181, 183, and 184.

Table 3-1. Casting Skull Dissolved During Each Experiment

Element	Concentration (wt %)	Exp. 181 Mass in 10.00 g	Exp. 183 Mass in 5.01 g	Exp. 184 Mass in 12.81 g
U	63.01	6.30	3.15	8.08
Er	5.40	0.54	0.27	0.69
Mo	2.47	0.25	0.12	0.32
Sn	0.01	0.001	0.0004	0.001

Due to the presence of graphite in the skull oxide (approximately 5 wt %), UDS were expected after dissolution. The mass of the filtered and washed solids collected following Exp. 181 (Figure 3-4) was 5.88 g after drying. The fluoride and Al added when it appeared the oxides had not completely dissolved likely contributed to a mass of UDS higher than anticipated. These solids were analyzed, and the elemental composition and masses (of interest) are shown in Table 3-2. The mass of the filtered and washed solids collected following Exp. 183 (Figure 3-5) was 0.18 g after drying. These solids were analyzed, and the elemental composition and masses are shown in Table 3-3. The mass of the filtered and washed solids collected following Exp. 184 (Figure 3-6) was 0.85 g after drying. These solids were analyzed, and the elemental composition and masses are shown in Table 3-4. The weight percentages of U, Er, and Mo in the solids were higher in the UDS from Exp. 183 than in Exp. 184. It is likely that the solids in Exp. 183 were not as well washed following filtration as those in Exp. 184, so U, Mo, and Er associated with interstitial liquid may have still been present in the solids.

Figure 3-4. Exp. 181 – Filtered/Washed/Dried Solids and Filter Paper

Table 3-2. Exp. 181 – Elemental Composition of Filtered/Washed/Dried Solids

Element	Concentration (wt %)	Mass (g)
U	0.51	0.030
Er	0.17	0.0098
Mo	0.03	0.0015
Sn	0.03	0.0016

Figure 3-5. Exp. 183 – Filtered/Washed/Dried Solids and Filter Paper

Table 3-3. Exp. 183 – Elemental Composition of Filtered/Washed/Dried Solids

Element	Concentration (wt %)	Mass (g)
U	7.08	0.013
Er	2.07	0.0037
Mo	0.25	0.00046
Sn	0.0022	0.000004

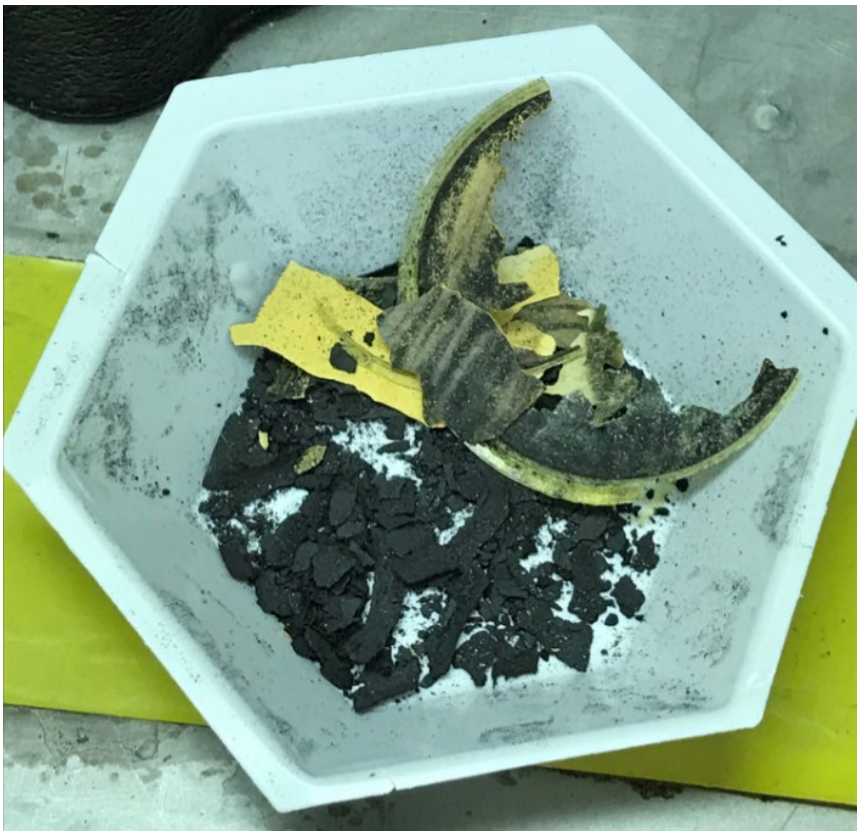

Figure 3-6. Exp. 184 – Filtered/Washed/Dried Solids and Filter Paper

Table 3-4. Exp. 184 – Elemental Composition of Filtered/Washed/Dried Solids

Element	Concentration (wt %)	Mass (g)
U	0.84	0.0072
Er	0.29	0.0025
Mo	0.05	0.0004
Sn	0.0009	0.000008

To complete the material balances around the skull oxide dissolutions, a sample of the filtrate from each experiment was analyzed by ICPMS. The elemental compositions and masses of interest are shown in Table 3-5, Table 3-6, and Table 3-7 for Exp. 181, 183, and 184, respectively. The measure volume of filtrate from each experiment was 300 mL (Exp. 181), 147 mL (Exp. 183), and 147 mL (Exp. 184).

Table 3-5. Exp. 181 – 20 g/L U Filtrate

Element	Concentration (g/L)	Mass (g)
U	19.60	5.88
Er	6.07	1.82
Mo	0.83	0.25
Sn	0.002	0.0006

Table 3-6. Exp. 183 – 20 g/L U Filtrate

Element	Concentration (g/L)	Mass (g)
U	20.45	3.01
Er	5.99	0.88
Mo	0.81	0.12
Sn	0.002	0.0003

Table 3-7. Exp. 184 – 50 g/L U Filtrate

Element	Concentration (g/L)	Mass (g)
U	53.18	7.80
Er	16.55	2.44
Mo	2.13	0.31
Sn	0.0051	0.0008

The material balance closure for each element was defined as the ratio of the mass of each element in the filtrate and UDS to the element in the skull oxide received from Y-12. The material balance closures for each experiment are shown in Table 3-8. The analysis of the skull oxide performed by the SRNL Analytical Characterization and Sample Management group (Table 3-1) was used as the basis for the mass of each element dissolved. The dissolution experiments showed that the U and other metals can be recovered by HNO_3 dissolution, but a majority of the graphite remains as UDS. Following dissolution of the skull oxide material, the solids will need to be filtered and washed with fresh dissolving solution to remove interstitial liquid containing dissolved U. Since the one sigma uncertainty associated with the ICPMS method is ±20%, the material balance closure for U is indistinguishable from 100%. The material balance closure for Er is greatly in excess of 100% for each dissolution; therefore, it appears that the Er concentration in the skull oxide measured at SRNL was either biased low or that the low bias was associated with nonhomogeneous sampling. The Exp. 181 material balance closure for Sn also greatly exceeds 100% which is attributed to the very high concentration of Sn measured in the UDS (compared to Exp. 183 and 184). For comparison, the characterization data obtained from the Y-12 analyses (Table 2-1) of the skull oxide was used as the source material for material balances. The material balance closures using the Y-12 analyses and SRNL analyses for the filtrate and undissolved solids are shown in Table 3-9. Using the Y-12 analyses, instead of the SRNL analysis, for the source skull oxide provides better closure for most of the material balances.

Table 3-8. Material Balance Closure for Skull Oxide Dissolutions using SRNL Analyses

Element	Material Balance Closure (%)		
	Exp. 181	Exp. 183	Exp. 184
U	94	96	97
Er	339(1)	327(1)	352(1)
Mo	101	97	99
Sn	295(2)	76	79

(1) High closure due to low bias in measured Er concentration in skull oxide material
(2) High closure due to high bias in measured Sn concentration in UDS

Table 3-9. Material Balance Closure for Skull Oxide Dissolutions using Y-12 Analyses

Element	Material Balance Closure (%)		
	Exp. 181	Exp. 183	Exp. 184
U	99	101	102
Er	92	88	95
Mo	110	105	108
Sn	369(1)	95	99

(1) High closure due to high bias in measured Sn concentration in UDS

3.1.3 U Recovery in the Filtrate Solutions and UDS

To specifically assess the efficiency of the dissolution processes in solubilizing the U in the skull oxide material, U recovery efficiencies in the filtrate solutions and the UDS were calculated for each experiment. The recovery efficiencies were calculated as the ratios of the U mass recovered in the filtrates (Table 3-5 (Exp. 181), Table 3-6, (Exp. 183), and Table 3-7 (Exp. 184)) and UDS (Table 3-2 (Exp. 181), Table 3-3 (Exp. 183), and Table 3-4 (Exp. 184)) to the total U recovered in both streams. The recovery efficiencies are shown in Table 3-10.

Table 3-10. U Recovery Efficiencies in the Filtrate Solutions and UDS

Exp.	U Recovery Efficiency (%)	
	Filtrate	UDS
181	99.49	0.51
183	99.58	0.42
184	99.91	0.09

The recovery efficiency data in Table 3-10 show that the majority of the U in the skull oxide material was soluble using the conditions specified for the 20 and 50 g/L dissolution flowsheets. The amount of U remaining in the UDS was less than approximately 0.5% in all of the dissolution experiments and was less than 0.1% for the experiment targeting a final U concentration of 50 g/L. The UDS following dissolution of the skull oxide can be discarded as a low level waste without any significant loss of U.

3.1.4 *Characterization of Offgas During Skull Oxide Dissolution*

The offgas generation rates for Exp. 183 and 184 in which the U-10Mo casting skull was dissolved to final U concentrations of 20 and 50g/L, respectively, are shown in Figure 3-7 and Figure 3-8. In both experiments, the offgas was primarily NO with no H_2 generation within detection limits, which is consistent with the dissolution of U oxides.[16] The Raman detection limit for H_2 in these runs was approximately 0.4 vol % due to noise in the signal, but even with this noise there were no consistent upward or downward trends indicating that H_2 was being generated. Therefore, there are no flammable gas concerns for the casting skull dissolution for this range of terminal U concentrations.

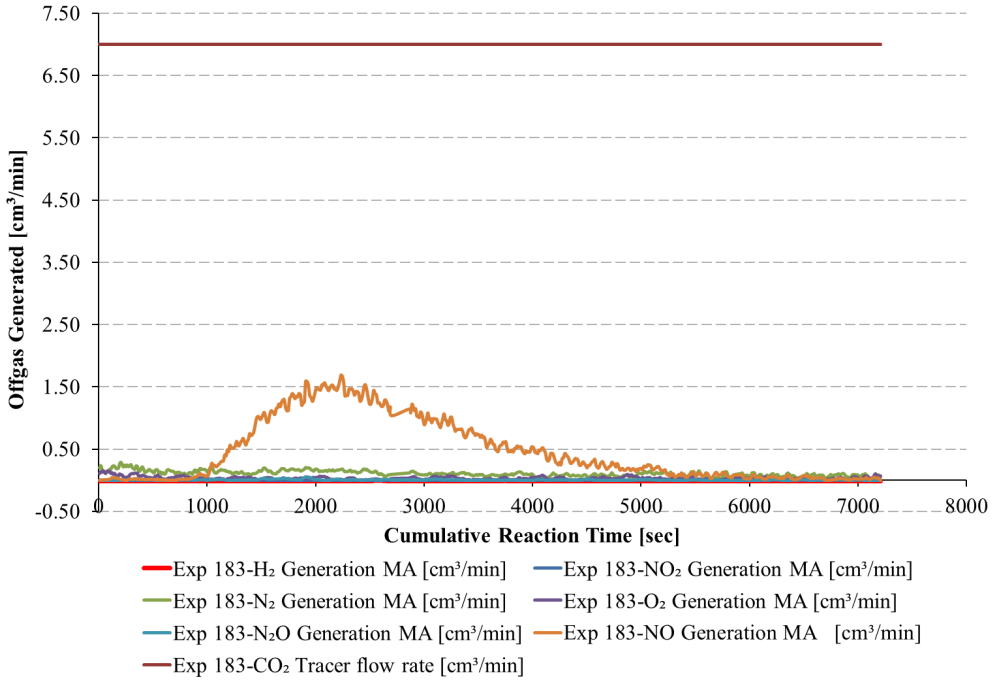

Figure 3-7. Exp. 183 – Offgas Generation Rates from Oxide Dissolution to 20 g/L U

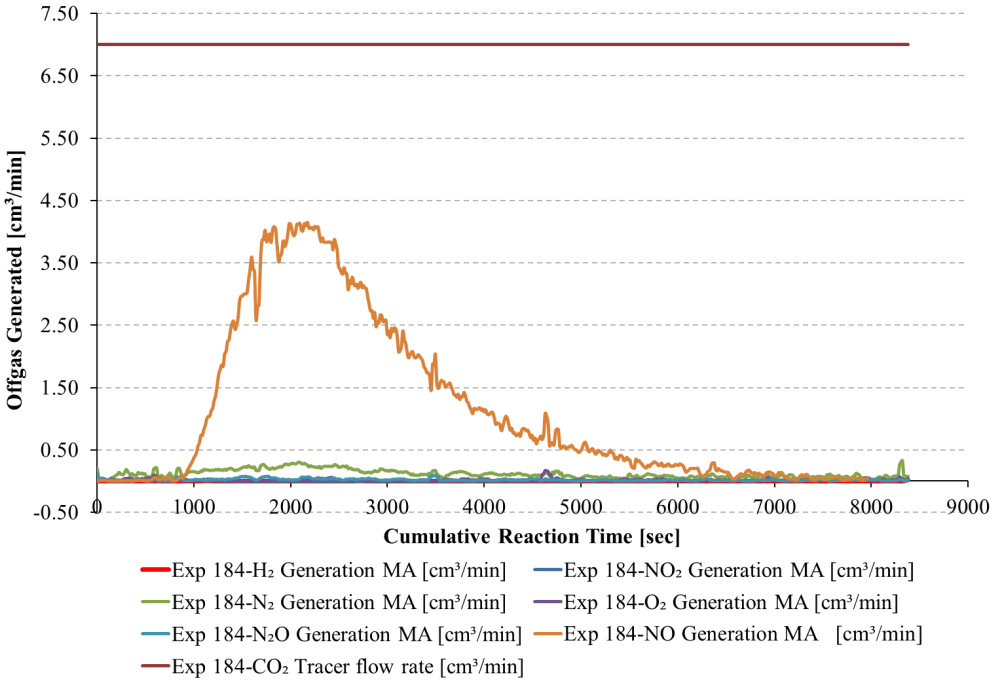

Figure 3-8. Exp. 184 – Offgas Generation Rates from Oxide Dissolution to 50 g/L U

Time zero in Figure 3-7 and Figure 3-8 corresponds to the start of heat-up from room temperature. In Exp. 183, the boiling point of the solution was reached after approximately 27 minutes. In Exp. 184, boiling was reached after approximately 24 minutes. Both experiments show that the maximum offgas generation

(of NO) occurs about 8 minutes after reaching boiling. Exp. 183 had a peak NO generation rate of approximately 1.5 cm^3/min (at 0° C and 1 atm) while Exp. 184 had a peak NO generation rate of approximately 4 cm^3/min. The ratio of the peak offgas rates for Exp. 184 to Exp. 183 is 2.67 which roughly matches the ratio of the masses of the casting skull used in the experiments (i.e., 2.56) showing that the peak offgas rate scales to the amount of material being dissolved.

While no NO_2, an orangish-brown gas, was observed in Exp. 183, there was visual evidence that NO_2 was present inside the dissolver head space during Exp. 184, but not in the condenser after reaching boiling. It is hypothesized that the condenser enabled the absorption of the NO_2 back into the solution through reactions 2 and 3, and released the measured NO.[17]

$$2\ NO_2(g) + H_2O(l) = HNO_2(l) + HNO_3(l) \quad (2)$$

$$3HNO_2(l) = HNO_3(l) + H_2O(l) + 2NO(g) \quad (3)$$

Equations 2 and 3 are combined to give equation 4 which summarizes the overall reaction.

$$3NO_2(g) + H_2O(l) = 2HNO_3(l) + NO(g) \quad (4)$$

4.0 Conclusions

Skull oxide from the casting operations used at Y-12 to produce U-10Mo ingots was dissolved using conditions based on optimized flowsheets developed for the dissolution of U-Mo-Zr foil and Al-clad U-Mo-Zr mini-plates to final U concentrations of 20 and 50 g/L. The flowsheet recommendations for the dissolution of the foil and mini-plates were based on the use of a sufficient volume of 4 M HNO_3 at the boiling point of the solution to achieve a final acid concentration greater than approximately 3.5 M when targeting either U concentration. For dissolutions targeting 50 g/L U, 0.5 M Fe (as $Fe(NO_3)_3$) should be added to the solution to prevent the precipitation of uranyl molybdate. Following dissolution of the skull oxide material, the UDS need to be filtered to remove the insoluble graphite from the solution and washed with fresh dissolving solution to remove interstitial liquid containing dissolved U.

Material balance and recovery efficiency data from the dissolution experiments show that the U in the skull oxide material was soluble using the conditions specified for the 20 and 50 g/L flowsheets. The UDS remaining from both prototypical dissolutions were 4-7% of the mass of the source material which was approximately equal to the amount of graphite in the skull oxide based on the Y-12 analysis (i.e., 5.1 wt %). Uranium material balance closures were nominally 100% and the amount of U remaining in the UDS was less than approximately 0.5% and was less than 0.1% for the experiment targeting a final U concentration of 50 g/L. The UDS following dissolution of the skull oxide can be discarded as a low level waste without any significant loss of U.

The offgas generation and composition from the skull oxide dissolutions were measured by Raman spectroscopy. There was no detectable H_2 in the offgas stream from the casting skull dissolutions which is consistent with the dissolution of U oxides. The offgas consisted of 100% NO (in an inert head space) with an approximate peak generation rate of 0.3 cm^3/min (0 °C, 1 atm) per gram of skull oxide. It took about 19 minutes to dissolve each gram of skull oxide for the dissolution targeting 20 g/L U and about 10 minutes to dissolve each gram of skull oxide targeting 50 g/L U based on the NO generation. The presence of the Fe in the solution likely increased the dissolution rate for the experiment targeting 50 g/L U.

5.0 Recommendations

Based on the experimental results, SRNL recommends using the same flowsheets for dissolving the casting skull which were demonstrated for the U-10Mo-Zr foils and the Al-clad U-10Mo-Zr mini-plates. The U

will readily leach from the skull oxide material. The UDS will need to be filtered and washed with fresh dissolving solution to minimize the loss of U to the interstitial liquid. The uranyl nitrate in the filtrate can then be purified using the solvent extraction flowsheets which were demonstrated for the foils and mini-plates[18] and converted into metal for recycle to the HPRR fuel fabrication process.

6.0 References

1. K. A. Dunn, G. L. Fredrickson, T. S. Rudisill, G. F. Vandegrift, and M. A. Williamson, *Uranium Recovery from Scrap Generated During Fabrication of USHPRR Fuel*, SRNL-TR-2017-00306, Savannah River National Laboratory, Aiken, SC (September 2017).
2. D. C. Stepinski, L. Maggos, J. Swanson, J. Stevens, and G. F. Vandegrift, *Scrap Recovery Operations in the Fuel Fabrication Capacity*, RERTR 2008 – 30th International Meeting on Reduced Enrichment for Research and Test Reactors, Washington, DC (October 2008).
3. D. C. Stepinski, J. Swanson, J. Stevens, and G. F. Vandegrift, *Dissolution of U-Mo-Alloy Scrap from Fuel Fabrication*, ANL/CSE-13/37, Argonne National Laboratory, Argonne, IL (2008).
4. J. Jerden, J. Fortner, and D. Stepinski, *Dissolution of Zirconium-Bonded Monolithic, Uranium-Molybdenum Fuel for Uranium Recovery*, ANL/SCE-13/30, Argonne National Laboratory, Argonne, IL (May 2009).
5. A. J. Youker, L. E. Maggos, D. C. Stepinski, A. J. Bakel, and G. F. Vandegrift, *Fuel Fabrication Capability (FFC) Scrap Recycle Report*, ANL/CSE-13/6, Argonne National Laboratory, Argonne, IL (September 2009).
6. A. J. Youker, D. C. Stepinski, L. E. Maggos, A. J. Bakel, and G. F. Vandegrift, *Aqueous processing of U-10Mo Scrap for high performance research reactor fuel*, J Nucl Mater, 427, p. 185-192 (2012).
7. A. J. Ziegler, L. E. Maggos, D. C. Stepinski, A. J. Bakel, and G. G. Vandegrift, *Scrap Recovery for Fabrication of U-10Mo fuel for High Performance Research Reactors*, RERTR – 31st International Meeting on Reduced Enrichment for Research and Test Reactors, Beijing, China (November 2009).
8. W. E. Daniel, T. S. Rudisill, and P. E. O'Rourke, *Dissolution Flowsheet for U-10Mo Scrap Generated from the Fabrication of High Performance Research Reactor Fuel*, SRNL-STI-2019-00531, Savannah River National Laboratory, Aiken, SC (September 2019).
9. P. Faugeras, C. Lheureux, and P. Leroy, *Etude De Solubilite Du Molybdene en Miliieu Nitrique*, CEA Report No.1823, Nuclear Study Center, Seclay, France (1961).
10. W. W. Schulz and E. M. Duke, *Reprocessing of Low-Enrichment Uranium-Molybdenum Alloy Fuels*, HW-62086, General Electric Company, Richland, WA (September 1959).
11. Baseline Change Request, *Scrap Recovery Solutions and Technology Maturation Options*, SRNL-L6000-2018-00017, Savannah River National Laboratory, Aiken, SC (April 4, 2018).
12. T. S. Rudisill and W. E. Daniel, *Task Technical and Quality Assurance Plan for the Development of Dissolution Flowsheets for Scrap Generated during Fabrication of U-Mo High Performance Research Reactor Fuel*, SRNL-RP-2018-01126, Savannah River National Laboratory, Aiken, SC (March 2019).
13. P. Tkac and A. Paulenova, *Speciation of Molybdenum (VI) In Aqueous and Organic Phases of Selected Extraction Systems*, Sep Sci Technol, 43:9-10, 2641-2657 (2008).
14. L. M. Ferris, *Grind-Leach Process for Graphite-Base Reactor Fuels that Contain Coated Particles: Laboratory Development*, ORNL-4110, Oak Ridge National Laboratory, Oak Ridge , TN (1967).
15. C. Rissom, H. Schmidt, and W. Voigt, *Crystal structure and thermal properties of a new double salt: $K_2SiF_6 \cdot KNO_3$*, Cryst Res Technol, 43, 74-82 (2008).
16. J. H. Gray, The Dissolution of Uranium Oxides in HB-Line Phase I Dissolvers, WSRC-TR-2003-00235, Westinghouse Savannah River Company, Aiken, SC (2003).
17. R. M. Counce, *The Scrubbing of Gaseous Nitrogen Oxides in Packed Towers*, ORNL-5676, Oak Ridge National Laboratory, Oak Ridge , TN (1980).
18. T. S. Rudisill and W. E. Daniel, *Purification of U from Scrap Generated during the Fabrication of U-Mo High Performance Research Reactor Fuel*, SRNL-STI-2021-00067, Savannah River National Laboratory, Aiken, SC (February 2021).

Distribution:

christopher.orton@srnl.doe.gov
jonathan.duffey@srnl.doe.gov
kerry.dunn@srnl.doe.gov
a.fellinger@srnl.doe.gov
dennis.vinson@srnl.doe.gov
lora.rousseau@srnl.doe.gov
eric.anderson@srs.gov
gene.daniel@srnl.doe.gov
tracy.rudisill@srnl.doe.gov
christopher.armstrong@srnl.doe.gov
harris.eldridge@srnl.doe.gov
jarrod.gogolski@srnl.doe.gov
eddie.kyser@srnl.doe.gov
michael.lee@srnl.doe.gov
charles.nash@srnl.doe.gov
robert.pierce@srnl.doe.gov
john.scogin@srnl.doe.gov
thomas.shehee@srnl.doe.gov
philip.almond@srnl.doe.gov
matthew.mills@srnl.doe.gov
Records Administration (EDWS)